NeuroImage 62 (2012) 930–937

Contents lists available at SciVerse ScienceDirect

NeuroImage

journal homepage: www.elsevier.com/locate/ynimg

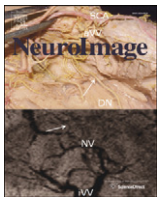

Review

Calibrated fMRI

Richard D. Hoge *

Depts. of Physiology, Radiology, and Biomedical Engineering, Université de Montréal, Montreal, Quebec, Canada
Center de recherche de l'institut de gériatrie de Montréal, Montreal, Quebec, Canada

ARTICLE INFO

Article history:
Accepted 9 February 2012
Available online 17 February 2012

Keywords:
Calibrated MRI
fMRI
Hypercapnia
Hyperoxia
BOLD
Oxygen
Metabolism

ABSTRACT

Functional magnetic resonance imaging with blood oxygenation level-dependent (BOLD) contrast has had a tremendous influence on human neuroscience in the last twenty years, providing a non-invasive means of mapping human brain function with often exquisite sensitivity and detail. However the BOLD method remains a largely qualitative approach. While the same can be said of anatomic MRI techniques, whose clinical and research impact has not been diminished in the slightest by the lack of a quantitative interpretation of their image intensity, the quantitative expression of BOLD responses as a percent of the baseline T2*- weighted signal has been viewed as necessary since the earliest days of fMRI. Calibrated MRI attempts to dissociate changes in oxygen metabolism from changes in blood flow and volume, the latter three quantities contributing jointly to determine the physiologically ambiguous percent BOLD change. This dissociation is typically performed using a "calibration" procedure in which subjects inhale a gas mixture containing small amounts of carbon dioxide or enriched oxygen to produce changes in blood flow and BOLD signal which can be measured under well-defined hemodynamic conditions. The outcome is a calibration parameter *M* which can then be substituted into an expression providing the fractional change in oxygen metabolism given changes in blood flow and BOLD signal during a task. The latest generation of calibrated MRI methods goes beyond fractional changes to provide absolute quantification of resting-state oxygen consumption in micromolar units, in addition to absolute measures of evoked metabolic response. This review discusses the history, challenges, and advances in calibrated MRI, from the personal perspective of the author.

Contents

Introduction

The term "calibrated MRI" was introduced by Tim Davis in 1998 (Davis et al., 1998) to describe a new method in which changes in the blood oxygenation-level dependent (BOLD) signal and cerebral blood flow (CBF) during hypercapnia could be used to "calibrate" the BOLD signal to yield a quantitative estimate of the relative change in oxygen consumption from subsequent BOLD and CBF measurements acquired during the execution of a task. Without such calibration, the BOLD signal used in countless functional studies is, despite its sensitivity, a largely qualitative index reflecting multiple physiological processes in a non-specific way. Calibrated MRI is thus of particular importance for the meaningful comparison of functional response amplitudes observed in subject cohorts in whom vascular and/or metabolic physiology may differ.

* 4565 Queen Mary, M6803, Montreal, Qc, Canada, H3W 1W5. Fax: +1 514 340 3548.
E-mail address: rick.hoge@linev.ca.

1053-8119/$ – see front matter © 2012 Elsevier Inc. All rights reserved.
doi:10.1016/j.neuroimage.2012.02.022

One way to describe calibrated MRI is by drawing a parallel with arterial spin-labeling MRI. In ASL, spatially targeted inversion prepulses are applied to the neck to create a flow-dependent contribution to the total MRI signal that is imaged. The small, flow-dependent component in a spin-labeled MRI scan is very much like the small, deoxyhemoglobin-dependent component of the T2*-weighted MRI signal discovered by Ogawa (Ogawa et al., 1990). The difference is that, with ASL, it is fairly easy to acquire a "control" acquisition which is identical to the labeled scan only lacking the flow-dependent component. Subtraction of the control from the labeled signal thus isolates the purely flow-dependent ASL difference signal. While the control signal in ASL can be obtained by simply turning off the labeling prepulse (taking care to to control for magnetization transfer), there is no similarly direct way to selectively disable the effect of deoxyhemoglobin on the T2*-weighted MRI signal (one could envision alternating between spin- and gradient-echoes, perhaps, but bulk susceptibility effects will be a challenge). In ASL, the ability to isolate the pure flow component is extremely useful, as the resultant difference signal is linearly proportional to the specific physiological parameter of blood flow. Calibrated MRI attempts to achieve the same thing with the BOLD signal, providing the signal component dependent purely on deoxyhemoglobin (dHb) at rest. This parameter was dubbed *M* in the original calibrated MRI paper by Davis, the letter chosen to indicate its equivalence to the (M)aximum possible increase in BOLD signal from a specific baseline. Changes in the dHb-dependent signal are close to linearly proportional to changes in the tissue concentration of hemoglobin, and a linear relationship can be achieved by factoring into terms representing blood volume and dHb concentration and applying an exponent slightly greater than unity to the latter term. Knowledge of task-induced changes in blood flow (from ASL) and tissue deoxyhemoglobin content (from calibrated BOLD) can then be used to estimate the corresponding change in oxygen consumption.

As noted above, there is no direct way to turn dHb-dependence on and off in MRI signals. One way to measure *M* directly would be to measure the signal change caused by eliminating all deoxyhemoglobin in tissues, which was in fact demonstrated by Ogawa using carbon monoxide in mice in the very first BOLD paper (Ogawa et al., 1990). Since this specific approach is clearly not applicable in human subjects, the original calibrated MRI technique described by Davis used hypercapnic vasodilation produced by breathing 5% CO_2 in air to achieve controlled, partial washout of venous dHb that could be extrapolated to the maximal BOLD response *M* using the signal model he proposed. While Davis's model expression is quite simple, it contains two parameters, α and β, which are not measured but rather assumed from literature estimates. The Davis approach also assumes that $CMRO_2$ does not change during hypercapnia, and that arterial blood is 100% saturated.

While variations on this scheme, based for example on hyperoxia, will be discussed below, it is important to emphasize that all current methods seek to provide a valid estimate of the resting BOLD signal *M* for subsequent normalization of task-induced BOLD changes. Some comments on the physical meaning of *M*, and comparison of values in different studies are thus warranted. As mentioned above, *M* is equivalent to the maximal possible BOLD signal that would be observed upon total elimination of all dHb from tissues. Typically *M* is expressed as a hypothetical percent signal change relative to the resting T_2*-weighted MRI signal, so a given value is really only meaningful for the specific echo-time, field strength, and macrovascular weighting applicable for that particular measurement. As long as the same conditions apply during measurement of task responses, $CMRO_2$ changes computed using that *M* value will be valid. However care must be taken in using or comparing *M* values derived under different measurement conditions.

History

Current interest in calibrated MRI stems largely from the problem of comparing BOLD responses between groups who may differ in their vascular and metabolic physiology, such as young and elderly cohorts, or healthy individuals vs. patients affected by vascular disease. However the initial development and application of calibrated MRI (Davis et al., 1998) targeted questions on the very nature of brain activation and the fundamental mechanisms of BOLD contrast.

While the origins of fMRI are discussed elsewhere in this issue, the emergence of calibrated MRI methods is inextricably linked with the search for a physiological interpretation of the BOLD fMRI signal. From the earliest descriptions by Ogawa et al. (Ogawa et al., 1990) of how T2*-weighted MRI signals are affected by paramagnetic deoxyhemoglobin in blood, the dynamic behavior of oxidative metabolism during increased neuronal activity was recognized as being of central importance in the BOLD phenomenon.

Positron emission tomography (PET) studies combining measures of cerebral blood flow (CBF) and the cerebral metabolic rate of oxygen consumption ($CMRO_2$) (Fox and Raichle, 1986; Fox et al., 1988) played an important role in the realization that the BOLD phenomenon arises because fractional changes in CBF during increased neuronal activity are generally larger than the corresponding fractional changes in $CMRO_2$ (Ogawa et al., 1993). While this explained the physical basis of the phenomenon, the physiological significance of this apparent disparity became the subject of intense debate during the early years of fMRI.

The above-mentioned debate was fueled largely by the paradox between the earliest PET studies (Baron et al., 1984; Raichle et al., 1976), which consistently portrayed substantial oxygen consumption in the brain, supplied through a tight regional proportionality in blood supply, and the PET studies of the late 1980's showing what was described as a focal temporal uncoupling between CBF and $CMRO_2$. The paradox was compounded by the fact that fractional changes in glucose uptake were found to be very similar to those of CBF (i.e. disproportionately large compared with $CMRO_2$ changes) during focal stimulation (Fox and Raichle, 1986). Initial interpretations on these results emphasized non-oxidative glucose consumption during brain activation, downplaying the role of oxidative metabolism in supporting transient increases in synaptic activity (Fox et al., 1988).

Given the paradox between the resting brain's critical dependence on oxygen, and what was considered to be a surprising failure to use this highly efficient source of cellular energy during physiological loading, numerous imaging studies throughout the 1990's sought to identify situations in which activation-induced increases in $CMRO_2$ might in fact be demonstrated. It was in this environment that I first became interested in calibrated MRI methods, as a Ph.D. student at the Montreal Neurological Institute (MNI) in 1994.

The imaging group at the MNI was actively involved in both the advancement of PET methodologies and in their application to a broad array of neuroscience questions (Coghill et al., 1994; Kuwabara et al., 1992; Ohta et al., 1992; Redies et al., 1989; Zatorre et al., 1992). A particularly exciting development was the emergence of new PET methods for imaging $CMRO_2$, using a single inhalation of ^{15}O, that were more manageable than previous methods requiring three separate image acquisitions (each with their own administration of an injected or inhaled tracer) and lasting up to 50 min. It was hoped that the shorter imaging times permitted by these new methods, on the order of three minutes, would be better suited to the dynamic monitoring of transient fluctuations in neuronal activity. One of the MNI's strengths has always been its ability to combine cutting edge imaging physics with advanced neuroscience concepts, and this was evidenced in an initiative led by Sean Marrett to construct visual stimulation patterns that would specifically target regions in

visual cortex endowed with high concentrations cytochrome oxidase (a key enzyme in oxygen metabolism) (Marrett and Gjedde, 1997).

Early work with such stimuli, in particular a yellow and blue radial checkerboard chosen because the combination of color and luminance contrast was expected to activate multiple visual pathways, produced a range of results with the new PET $CMRO_2$ methods. Of particular note was a study conducted by Manouchehr Vafaee at the MNI (carried out in 1997 and published in 1999 (Vafaee et al., 1999)), who found an intriguing dependence between the evoked $CMRO_2$ response and the temporal modulation frequency of the yellow/blue checkerboard, with a sharp rise in oxygen consumption (to approximately 118% of baseline) at a frequency of 4 Hz but with little or no change at virtually all other frequencies (1–50 Hz).

Because PET CBF studies of other visual stimuli (Fox and Raichle, 1984) reported a peak blood flow response at higher frequencies, the Vafaee results suggested that there might be a highly variable proportionality between fractional changes in CBF and $CMRO_2$ with visual stimulation frequency. Having recently become interested in studying the physiological basis of BOLD fMRI with arterial spin-labeling (ASL), I recognized immediately that such variable coupling should produce highly distinctive effects in the relationship between jointly measured ASL and BOLD signals.

While we initially intended to make inferences about CBF–$CMRO_2$ coupling simply by plotting ASL–BOLD relationships measured during systematic variations in visual stimulation parameters like contrast and frequency, the class of techniques that came to be known as calibrated MRI was also taking shape at the Massachusetts General Hospital NMR Center (MGH-NMR) around that time (Davis et al., 1998; Mandeville et al., 1999). Calibrated MRI, which promised to translate our ASL–BOLD curves into actual $CMRO_2$ measures, seemed like the perfect complement to the single-inhalation PET $CMRO_2$ work in progress at the MNI.

Early applications

While we were never able to replicate the wide variations in CBF–$CMRO_2$ coupling implied by the MNI PET work on frequency dependent responses, hypercapnically calibrated MRI opened a number of intriguing possibilities and questions. The calibrated MRI study I carried out in the course of my Ph.D. project suggested a more predictable and linear coupling between CBF and $CMRO_2$ in visual cortex for a broad range of visual stimuli designed to target many different visual pathways (both rich and poor in oxidative enzymes). To the extent that we were able to replicate the stimulation conditions of the more focused single-inhalation PET studies (i.e. those in which all averaging and radiation dose were devoted to a single stimulus type), the results obtained with calibrated MRI were in very close agreement with those from PET (both methods indicated a 25% increase in $CMRO_2$ for the now infamous yellow/blue checkerboard at maximal contrast) (Hoge et al., 1999b; Marrett and Gjedde, 1997). Regardless of the visual stimulus characteristics, all flow and metabolism responses appeared to be linearly coupled in a ratio of approximately 2:1 (Hoge et al., 1999b). At the time, we hoped that this simple CBF–$CMRO_2$ coupling relationship could be useful in BOLD signal modeling similarly to the power law relationship between CBF and CBV identified by Grubb (Grubb et al., 1974).

While the consistent linearity of the coupling curves and the agreement with PET under maximal stimulus conditions were encouraging, I was fascinated by the physical meaning of the calibration model introduced by Davis. Was this just a mathematical sleight-of-hand that happened to give a plausible answer under the right conditions? I felt the model could also be used to generate testable hypotheses about BOLD signal behavior that might be used to investigate the validity of the model and generate previously unobserved phenomena, ideas that ended up shaping my Ph.D. research.

One very satisfying experiment that stemmed from this direction was the adjustment of visual stimulus contrast, based on extensive pilot data we had acquired, to match the CBF increases produce by a set of graded hypercapnic manipulations. This allowed the direct comparison of oxygenation-dependent MR signals during neuronal stimulation and what we believed to be the metabolically inert condition of hypercapnia. The data revealed a dramatic drop in the BOLD signal level associated with neuronal stimulation compared with that caused by hypercapnia at the same level of CBF. We interpreted this visible (in time course plots) signal drop as direct evidence of increased oxygen metabolism during neuronal stimulation. While the accuracy of ASL measurements during hypercapnia and the impact of the latter manipulation on cellular metabolism and cerebral blood volume have been debated, the BOLD–CBF trends observed have been readily replicated and the overall validity of the Davis approach has been well supported by subsequent work (Chiarelli et al., 2007a; Kida et al., 2000; Leontiev and Buxton, 2007).

A second experiment was to test the hypothesis that ASL–BOLD relationships measured during graded hypercapnia administered at different levels of neuronal stimulation should produce a set of parallel curves whose separation reflects the relative difference in oxygen metabolism rate between the stimulation conditions. The data points acquired in this procedure traced out trajectories we termed iso-$CMRO_2$ contours, with a regular spacing and non-linear curvature that closely matched the characteristics predicted by the hypercapnic calibration model (Davis et al., 1998; Hoge et al., 1999a). While the two experiments described above were largely qualitative, we felt that they provided a compelling demonstration of the ideas underlying the Davis model. Our conclusion that these data demonstrated an increase in oxygen metabolism during neural stimulation was bolstered by other independent measures that emerged during this period, notably those based on optical imaging of intrinsic signals (Malonek et al., 1997). It should be noted that the majority of these early experiments were conducted using primary visual and motor stimulation. Later studies found similar results using cognitive tasks ranging from executive function (Goodwin et al., 2009) to memory encoding (Restom et al., 2008).

Challenges

Buoyed by what we felt was a successful proof-of-concept entering the new decade in 2000, I joined other members of the neuroimaging community in undertaking the enhancements and further validation needed to bring the calibrated MRI approach to a broader range of applications and users. While interest has remained strong in this area, broad adoption was initially slowed due to a number of challenges. This is not to say that there haven't been important initiatives to apply calibrated MRI to broader neuroscience questions; the group at UCSD led by Rick Buxton has applied the Davis model in numerous calibrated MRI studies exploring questions on the effects of caffeine on cerebral vasculature and aging (Ances et al., 2009; Perthen et al., 2008). This group has also examined flow-metabolism coupling in medial temporal lobe during a memory encoding task (Restom et al., 2008). In collaboration with the UCSD group, Beau Ances at Washington University has applied calibration methods to the study of neurological changes in HIV/AIDS (Ances et al., 2011). In the UK, the research team led by Laura Parkes has been active in applying the hyperoxic variant of calibrated MRI (described below) in the study of executive function in aging (Goodwin et al., 2009; Mohtasib et al., 2012). It's encouraging to note that many of these studies are quite recent as of 2011, and the resurgent interest in applications has occurred in tandem with renewed efforts to advance the theoretical and methodological basis of calibrated MRI (Gauthier and Hoge, 2011a; Griffeth and Buxton, 2011). Here we discuss some of the key

challenges, and how different groups have contributed in overcoming these.

Validating the accuracy of $\Delta\%CMRO_2$ estimates obtained using the Davis model, and that of associated $\Delta\%CBF$–$\Delta\%CMRO_2$ coupling relationships, has been a concern since the earliest applications discussed above (Chiarelli et al., 2007b; Leontiev and Buxton, 2007; Leontiev et al., 2007). While the beauty of this model is its simplicity, it is understood to be unrealistic in many details (Griffeth and Buxton, 2011; Obata et al., 2004).

The longest standing concerns have related to the question of what values to choose for the constants α and β in the Davis model. The parameter α is used to express cerebral blood volume (CBV) changes as a function of blood flow changes. Although the initial method used the value $\alpha = 0.38$ proposed by Grubb for total arterio-venous blood volume (Grubb et al., 1974), what is really required is the volume of the compartment in which deoxyhemoglobin resides — usually the venous circulation. Recent studies have used specialized methods to estimate a value of α appropriate for venous CBV, for example $\alpha = 0.18$ as in Chen et al. (Chen and Pike, 2010b). Moreover the introduction of MRI-based methods for measuring functional changes in CBV, such as imaging of vascular space occupancy (VASO) (Lu et al., 2003) may alleviate the need for modeling CBV in terms of CBF. However VASO requires a dedicated measurement scan, unlike ASL and BOLD which can be acquired simultaneously. Moreover VASO is likely to reflect total plasma volume, which is not the same as the venous fraction required for calibrated MRI. An additional debate has centered around whether CBV–CBF coupling is the same during both hypercapnic and task-induced increases in perfusion, although recent evidence suggests that the venous compartment behaves similarly in both cases (Chen and Pike, 2010b).

The parameter β, reflecting the non-linearity of R_2^*–[dHb] coupling, has generally been assigned a value of 1.5, based on phantom measurements and Monte Carlo simulations carried out (coincidentally) at 1.5 T (Boxerman et al., 1995a, 1995b; Weisskoff et al., 1994). Because the majority of calibrated MRI studies are currently carried out at 3 T, and more can soon be expected at 7 T, it will be important to re-evaluate the selection of this parameter as well. It has long been asserted that R_2^*–[dHb] coupling is likely to become more linear at higher field strengths, but this remains to be demonstrated experimentally. Because a strict interpretation of the Davis model requires BOLD signals in calibrated MRI to include only extravascular signals, it is understood that β should be in practice be considered as a "lumped constant" that accurately captures the mixed intra- and extra-vascular signals typically obtained in reality. The same can be said of α, given the true complexities of deoxyhemoglobin compartmentalization in the brain. In a recent paper, Griffeth et al. have argued that the original interpretations of α and β should be relaxed to combined the effects of multiple processes, and carried out numerical optimizations suggesting that the values $\alpha = 0.14$ and $\beta = 0.91$ might be more appropriate for the measurement conditions considered (Griffeth and Buxton, 2011).

Another interesting (and important) question that has arisen is whether $CMRO_2$ is really unchanged during the hypercapnic manipulations used in calibrated MRI. At high doses, CO_2 is known to exert an anesthetic effect in higher organisms although the exact dose dependence (presumably sigmoidal) is not well characterized in humans. Moderate to high doses of CO_2 also produce a perceptible sensation of air hunger in most individuals, which results in activation of brain structures associated with respiratory sensation, anxiety, and thoracic motor control (Evans et al., 2002). While anesthetic or sensory effects will very likely alter $CMRO_2$ in affected brain areas, it is not clear to what extent very low doses of CO_2 exert a generalized effect on $CMRO_2$ throughout the brain. To reliably dissociate such generalized effects from specific sensory or affective responses would require a carefully designed placebo-controlled study in which subjects are blind to the presence of CO_2. Currently a variety of findings on this topic have been reported including increases (Horvath et al., 1994; Jones et al., 2005) and decreases (Xu et al., 2011; Zappe et al., 2008) and no change (Chen and Pike, 2010a; Hino et al., 2000; McPherson et al., 1991). Although my group has tested relatively high concentrations of CO_2 (7–10%, up to 10 mm Hg increase in end-tidal CO_2), the approach we currently advocate for general research applications emphasizes the use of lower levels of CO_2 (5%, $\Delta ETCO2 \leq 5$ mm Hg) under conditions where subjects will ideally be unaware of the hypercapnic state (e.g. liberal gas flow rates supporting volitional increases in minute ventilation). Under such conditions, and given the converging agreement between hypercapnically determined M values and those measured directly, the bias from CO_2-induced changes in $CMRO_2$ in calibrated MRI is likely to be minimal. Such lower levels of hypercapnia are evidently more comfortable for patients as well.

A notable practical challenge, evident since our earliest experiments, has been that arterial spin-labeling of hypercapnic challenges tends to produce data of marginal quality. A large part of the reason why BOLD continues to be favored over ASL in fMRI mapping applications is simply that the signal-to-noise ratio in ASL is very low. On top of this, the functional contrast in pulsed ASL methods turns out to depend strongly on consistent control of label timing parameters which may be skewed during global flow increases (Buxton et al., 1998; Wong et al., 1998). While modern pulsed ASL methods incorporate controls for label timing (Luh et al., 1999; Wong et al., 1997), the optimization of these for calibrated MRI has proven challenging (Tancredi et al., In Press). Recent developments in continuous and pseudo-continuous ASL have helped to mitigate this issue (Chen et al., 2011; Fernandez-Seara et al., 2008; Wu et al., 2007, 2009), but further investigation is required to understand the effects of global flow increases on the labeling efficiency of these methods (Aslan et al., 2010). Another promising avenue for improving ASL sensitivity is correction of physiological noise (Glover et al., 2000). Wu et al. have demonstrated substantial improvements in ASL signal stability through RETROICOR modeling of cardiac pulsation (particularly for pulsed ASL) and respiratory movements (most notably for continuous ASL) (Wu et al., 2009).

Solutions and advances

As noted above, the promise of calibrated MRI methods has been offset by unresolved questions about their general applicability and the technically challenging nature of the procedures involved. Fortunately a number of elegant solutions to many of these issues have emerged.

A clever variation on the Davis hypercapnia approach was introduced in 2007 by Peter Chiarelli, Daniel Bulte, and colleagues at Oxford (Chiarelli et al., 2007c). In their adaptation, hypercapnia was replaced by hyperoxia which was induced by having subjects breathe enriched O_2 (typically 50–100% as compared with 21% in normal air). Rather than modeling venous dHb in terms of a change in blood flow, as done in the hypercapnic approach, the new method expressed dHb concentration in terms of changes in arterial O_2 content, which can be determined from changes in end-tidal O_2 prior to and during the hyperoxic manipulation. Because changes in blood flow are small and thus play very little role in the BOLD signal changes measured during this calibration, the importance of ASL is greatly diminished in this technique. Potential concerns about CO_2-induced changes in $CMRO_2$ are also alleviated, and hyperoxia is virtually imperceptible to subjects and thus generally more comfortable than hypercapnia. One new pitfall introduced is that a constant value of resting oxygen extraction fraction (OEF_0) must be assumed. While OEF_0 does appear to be quite constant throughout the brain in healthy individuals (Frackowiak et al., 1980), significant regional and inter-subject

variability has been demonstrated in cases of pathology (Baron et al., 1981; Yasaka et al., 1998).

While the hyperoxia method described above offers a number of advantages, its validity is subject to many of the same questions as the hypercapnic method. A succinct way of asking whether these methods are valid is to ask whether the values of *M* provided truly represent the resting (or conversely maximal) BOLD signal. The decade since calibrated MRI was introduced has seen a very wide range of reported *M* values. My own early studies described values extrapolated from hypercapnia of 15–;22% of the baseline T2*-weighted signal (Hoge et al., 1999a), which have always seemed implausibly large next to the 2% "rule-of-thumb" maximum commonly assumed for "real" task-evoked BOLD signals. However it is important to emphasize that *M* values are proportional to the echo-time used, which was 50 ms in these early 1.5 T experiments. Corrected for the currently common echo-time of 30 ms used (albeit generally at 3 T), the adjusted mean *M* value from those studies becomes 11.1%. This is still high compared with later values, and may reflect macrovascular weighting inherent in the ROI delineation procedures used. In the original Davis report (Davis et al., 1998), a group average *M* value of $7.9 \pm 0.7\%$ was reported. However BOLD acquisitions in that study used an asymmetric spin-echo sequence with an effective gradient-echo time of only 25 ms (moreover this sequence was believed to de-emphasize macrovessel responses). More recent studies at the currently popular field strength of 3 T have reported *M* values ranging from 5.3 to 12.1% (corrected to TE = 30 ms (Gauthier et al., 2011)), with a median value of 7.3%.

Due perhaps to what were perceived as very high *M* values in these initial reports, there has been some skepticism as to whether *M* represents a physically meaningful quantity that might actually be encountered in reality. To address this issue, my own graduate student Claudine Gauthier carried out a simple but effective study in which she had subjects breathe 10% CO_2 with a balance of 90% O_2 (carbogen) to drive venous saturation to extremely high levels (Gauthier et al., 2011) while BOLD signals were measured using conventional methods. The average BOLD signal change observed with this method, which does not depend on model parameters or the assumption of constant $CMRO_2$, was $7.5 \pm 1.0\%$. Although ASL and end-tidal O_2 measurements were not systematically acquired in these subjects, susceptibility-weighted imaging (SWI) indicated that a near-complete "arterialization" of venous blood was achieved. Measurements obtained in different subject groups to characterize this manipulation suggested that the venous O_2 saturation was likely to have exceeded 90% with this manipulation. Integrating measures from different groups in these followup measurements suggested that the "true" *M* at 100% venous saturation might be as high as 9.5%. However a subsequent study with all measures (BOLD, ASL, ETO_2) acquired simultaneously (Gauthier and Hoge, 2011a), along with SWI of a range of gas mixes, ultimately led us to believe that the 7.5% BOLD increase measured directly during the $10\%CO_2/90\%O_2$ carbogen mixture used in Gauthier et al. (2011) was in fact very close to the maximal value. This conclusion is further supported by the almost total elimination of the response produced by intense visual stimulation applied during the latter carbogen manipulation.

An outcome of our work with carbogen was that we had to adapt the Oxford hyperoxia model, which was originally derived for conditions leading to little or no change in CBF. Fortunately a simple modification to incorporate CBF into the modeling of blood O_2 content resulted in a generalized expression linking BOLD, CBF, and end-tidal O_2 that is exact for arbitrary combinations of hypercapnic flow increase and hyperoxic increases in arterial O_2 content. This Generalized Calibration Model (GCM) was subsequently compared (using carbogen with a lower CO_2 content) with the original hypercapnic and hyperoxic approaches, and found to provide *M* maps that were on average comparable to those of the Davis method but with better stability in the presence of noisy CBF signals (Gauthier and Hoge, 2011a). Interestingly, the hyperoxia method yielded maps of *M* in which the values tended to be significantly lower and more homogeneous than those seen in the other two methods. This appeared to reflect an absence of response in large veins, which typically lead to focal hot spots in BOLD activation maps. We were also able to show that the GCM reduced exactly to the Davis and Chiarelli–Bulte models under the respective assumptions of those models.

In our most recent extension of the above methods, we have shown that the GCM can be used to process data acquired during separate hyperoxic and hypercapnic manipulations to yield both the calibration parameter *M* and resting OEF. In this approach, which we have dubbed QUO_2 (for QUantitative O_2), data from each gas manipulation is substituted into the GCM without constraining OEF_0 to a specific value. While this does not give a unique value of *M* for a single manipulation (e.g. hyperoxia), *M* can nonetheless be expressed as a function of the variable OEF_0. Adding the second manipulation (e.g. hypercapnia) results in a different *M* vs. OEF_0 function and the resultant system of two equations can be easily solved for the unique solution of the two unknowns *M* and OEF_0. The technique also yields arterial O_2 content (as in the original Chiarelli–Bulte method) and resting CBF, which can be multiplied by the OEF_0 value at each voxel to provide maps of resting $CMRO_2$ in micromolar units (Gauthier and Hoge, 2011b). A satisfying aspect of this approach is that, by integrating previous hypercapnic and hyperoxic methods in a generalized model, it completes the "full circle" with early PET methods by allowing calibrated MRI to also measure both task-evoked responses and absolute resting baseline values. A related approach to imaging resting $CMRO_2$ was recently published by Dan Bulte, who showed that it was possible to determine *M* using the Davis approach, and then substitute this value into the Chiarelli–Bulte hyperoxia model to solve for resting OEF (Bulte et al., 2011). Another innovation introduced in the latter paper was the use of multiple post-ASL delay times during the gas calibration scans, which is likely to give superior sensitivity and accuracy during the global flow changes involved.

Fig. 1 illustrates the similarities and differences between the Davis and Chiarelli–Bulte models and the GCM using data from Gauthier and Hoge (2011b). In Fig. 1a, the set of three *M* vs. OEF_0 curves plotted for hyperoxia, hypercapnia, and combined hyperoxia-hypercapnia (carbogen breathing) is shown. The curves, which were generated from group average measurements of end-tidal O_2 and gray-matter MRI values, can be seen to intersect at a unique point whose coordinates give the actual values for *M* and resting OEF. For comparison, the *M* vs. OEF_0 curve implied by the Davis model is shown (dashed blue line). The Davis model does not include an OEF_0 term, assuming simply that all venous deoxyhemoglobin is generated through metabolism (i.e. arterial hemoglobin saturation is constant at 100%). The black GCM curve for hypercapnia can be seen to approach the Davis model, asymptotically, at high values of OEF_0. This reflects the fact that, at high levels of metabolic oxygen extraction, the impact of any deoxyhemoglobin arriving via incompletely saturated arterial blood becomes negligible (approaching the assumption of the Davis model). However at low values of OEF_0, there is considerable divergence between the Davis model and GCM for hypercapnic data due to an increase in the relative importance of arterial deoxyhemoglobin. While the GCM-based solution for *M* and OEF_0 is given by the intersection of the three GCM curves, the solution coordinates given by the method described by Bulte in Bulte et al. (2011) would be shifted slightly upward and to the right, since the Davis model is used (at the PaO_2 values seen in young healthy subjects, the GCM curve for hyperoxia is virtually identical to that obtained using the Chiarelli-Bulte model). Figs. 1b–c compare the Chiarelli–Bulte formulation and GCM in modeling the *M* vs. OEF_0 curve based on data acquired during carbogen inhalation, which causes simultaneous increases in arterial O_2 content and cerebral blood flow. Due to approximations in the original Chiarelli–Bulte

formula, it tends to progressively underestimate *M* when arterial O_2 saturation decreases below 100%, particularly when cerebral blood flow also increases (the reduced saturation shown here is simulated from real data). The effect of this would be a modest error in $CMRO_2$ at arterial hemoglobin saturations under 95%. The Davis and Chiarelli–Bulte models are thus special cases of the GCM that provide reasonable accuracy under the physiological conditions prevailing in young healthy volunteers. The GCM is nonetheless likely to better model the biophysics of BOLD contrast in populations with impaired cardiovascular or pulmonary function.

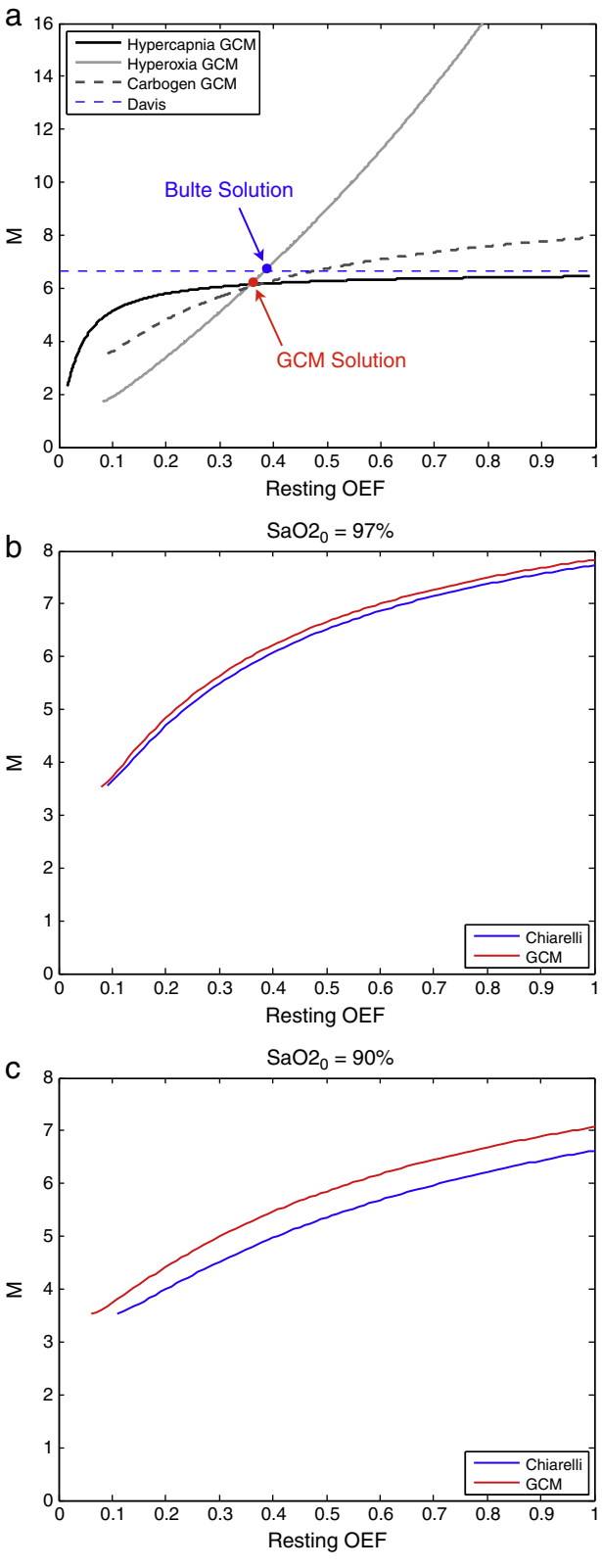

Fig. 1. Comparison of different calibrated MRI models. (a) Curves showing unconstrained *M* vs. OEF_0 relationships computed using the GCM for hypercapnia (solid black), hyperoxia (solid gray), and carbogen breathing (dashed gray) with BOLD and CBF data averaged within cortical gray matter. The three curves intersect at a well defined point, providing a readout of the actual *M* and OEF_0 values (red spot). The *M* value computed from the hypercapnia data using the Davis model is shown as the dashed blue line (not dependent on OEF_0). It can be seen that the hypercapnic GCM curve approaches asymptotically the constant limiting *M* value given by the Davis model. At the high arterial O_2 saturations typically seen in young healthy volunteers, the curves given for hyperoxia by the GCM and the Chiarelli–Bulte calibration model are virtually identical. The solution coordinates yielded by the calibration approach recently proposed by Bulte et al. are given by the intersection of the constant Davis *M* value and the hyperoxia curve (blue dot). (b–c) The differences between the GCM and Chiarelli–Bulte calibration expression are most pronounced when arterial O_2 saturation is significantly less than 100% and when cerebral blood flow increases substantially during the calibration procedure. The curves plotted show *M* vs. OEF_0 curves based on data acquired during carbogen inhalation, with simulated reductions in arterial O_2 saturation.

Foundations and the future

This review would not be complete without considering the earliest hypercapnia studies that are the predecessors of calibrated MRI, as well as some exciting future directions which diverge from the gas-calibration methods discussed here.

One of the first studies, carried out by Peter Jezzard and notable for combining optical and MRI measures, described blood saturation and BOLD effects in cats during respiratory manipulations including hypercapnia (Jezzard et al., 1994). One of the first human studies was published by Peter Bandettini, who showed that maps of the BOLD response to hypercapnia represented the spatial pattern of potential contrast in a way that could be used to normalize task-elicited responses so that they might better reflect the underlying magnitude of the neuronal response (Bandettini and Wong, 1997). While not seeking to quantify a specific physiological parameter, the method described by Bandettini nonetheless contains many of the central elements of calibrated MRI.

Notable among the newer techniques is quantitative BOLD (qBOLD), which uses model MR signals under the static dephasing regime to determine baseline hemodynamic parameters from a GESSE signal (He and Yablonskiy, 2007; He et al., 2008). The qBOLD method stems from earlier pioneering work on susceptibility effects in MRI signal, carried out by Yablonskiy and Haacke (1994 which, while discussed elsewhere in this issue, must also be acknowledged here. Another innovative approach, dubbed QUIXOTIC, was recently proposed by Div Bolar (Bolar et al., 2011). QUIXOTIC uses velocity-sensitive ASL to target directly the oxygenation signal from small venules. By specifically measuring the signal from this compartment, a localized measure of oxygen extraction and metabolism can be obtained. Another promising approach for calibrated functional MRI, recently published by Nicholas Blockley of UCSD (Blockley et al., 2011), is based on the idea that venous deoxygenated hemoglobin likely accounts for a significant fraction of the reversible component of transverse relaxation described by the rate constant R_2' ($1/T_2'$). Determining R2′ using an asymmetric spin-echo acquisition and computing the BOLD signal increase that would be observed if this component were reduced to zero may thus provide a means of determining *M* without requiring a gas calibration. Encouragingly, values for *M* obtained using this approach were consistent with those obtained using hypercapnic calibration under the Davis model.

Conclusion

Since the original introduction of the Davis model, calibrated MRI has advanced our understanding of BOLD contrast mechanisms and brain physiology. No longer limited to relative changes in $CMRO_2$ during task activation, the current generation of calibrated MRI techniques also provides a rich array of physiological information including resting oxygen extraction fraction and, by extension, resting oxygen metabolism in absolute micromolar units. Considering that these procedures also yield absolute resting CBF and CO_2- mediated vascular reactivity, calibrated MRI is poised to become a powerful diagnostic tool for characterizing physiological changes in aging and disease.

Acknowledgments

This research has been supported by numerous funding agencies, including the Canadian Institutes of Health Research, the Whitaker Foundation, the US National Institutes of Health, Canadian National Sciences and Engineering Research Council, the Canadian Foundation for Innovation, and the Ministère du développement économique, innovation et exportation du Québec. I would also like to thank the many scientific collaborators whose involvement has been critical in this work.

References

Ances, B.M., Liang, C.L., Leontiev, O., Perthen, J.E., Fleisher, A.S., Lansing, A.E., Buxton, R.B., 2009. Effects of aging on cerebral blood flow, oxygen metabolism, and blood oxygenation level dependent responses to visual stimulation. Hum. Brain Mapp. 30, 1120–1132.

Ances, B., Vaida, F., Ellis, R., Buxton, R., 2011. Test-retest stability of calibrated BOLD-fMRI in HIV − and HIV + subjects. NeuroImage 54, 2156–2162.

Aslan, S., Xu, F., Wang, P.L., Uh, J., Yezhuvath, U.S., van Osch, M., Lu, H., 2010. Estimation of labeling efficiency in pseudocontinuous arterial spin labeling. Magn. Reson. Med. 63, 765–771.

Bandettini, P.A., Wong, E.C., 1997. A hypercapnia-based normalization method for improved spatial localization of human brain activation with fMRI. NMR Biomed. 10, 197–203.

Baron, J.C., Bousser, M.G., Rey, A., Guillard, A., Comar, D., Castaigne, P., 1981. Reversal of focal "misery-perfusion syndrome" by extra-intracranial arterial bypass in hemodynamic cerebral ischemia. A case study with 15O positron emission tomography. Stroke 12, 454–459.

Baron, J.C., Rougemont, D., Soussaline, F., Bustany, P., Crouzel, C., Bousser, M.G., Comar, D., 1984. Local interrelationships of cerebral oxygen consumption and glucose utilization in normal subjects and in ischemic stroke patients: a positron tomography study. J. Cereb. Blood Flow Metab. 4, 140–149.

Blockley, N.P., Griffeth, V.E., Buxton, R.B., 2011. A general analysis of calibrated BOLD methodology for measuring CMRO(2) responses: comparison of a new approach with existing methods. NeuroImage 60, 279–289.

Bolar, D.S., Rosen, B.R., Sorensen, A.G., Adalsteinsson, E., 2011. QUantitative Imaging of eXtraction of oxygen and TIssue consumption (QUIXOTIC) using venular-targeted velocity-selective spin labeling. Magn. Reson. Med. 66, 1550–1562.

Boxerman, J.L., Bandettini, P.A., Kwong, K.K., Baker, J.R., Davis, T.L., Rosen, B.R., Weisskoff, R.M., 1995a. The intravascular contribution to fMRI signal change: Monte Carlo modeling and diffusion-weighted studies in vivo. Magn. Reson. Med. 34, 4–10.

Boxerman, J.L., Hamberg, L.M., Rosen, B.R., Weisskoff, R.M., 1995b. MR contrast due to intravascular magnetic susceptibility perturbations. Magn. Reson. Med. 34, 555–566.

Bulte, D.P., Kelly, M., Germuska, M., Xie, J., Chappell, M.A., Okell, T.W., Bright, M.G., Jezzard, P., 2011. Quantitative measurement of cerebral physiology using respiratory-calibrated MRI. NeuroImage 60, 582–591.

Buxton, R.B., Frank, L.R., Wong, E.C., Siewert, B., Warach, S., Edelman, R.R., 1998. A general kinetic model for quantitative perfusion imaging with arterial spin labeling. Magn. Reson. Med. 40, 383–396.

Chen, J.J., Pike, G.B., 2010a. Global cerebral oxidative metabolism during hypercapnia and hypocapnia in humans: implications for BOLD fMRI. J. Cereb. Blood Flow Metab. 30, 1094–1099.

Chen, J.J., Pike, G.B., 2010b. MRI measurement of the BOLD-specific flow-volume relationship during hypercapnia and hypocapnia in humans. NeuroImage 53, 383–391.

Chen, Y., Wang, D.J., Detre, J.A., 2011. Test–retest reliability of arterial spin labeling with common labeling strategies. J. Magn. Reson. Imaging 33, 940–949.

Chiarelli, P.A., Bulte, D.P., Gallichan, D., Piechnik, S.K., Wise, R., Jezzard, P., 2007a. Flow-metabolism coupling in human visual, motor, and supplementary motor areas assessed by magnetic resonance imaging. Magn. Reson. Med. 57, 538–547.

Chiarelli, P.A., Bulte, D.P., Piechnik, S., Jezzard, P., 2007b. Sources of systematic bias in hypercapnia-calibrated functional MRI estimation of oxygen metabolism. NeuroImage 34, 35–43.

Chiarelli, P.A., Bulte, D.P., Wise, R., Gallichan, D., Jezzard, P., 2007c. A calibration method for quantitative BOLD fMRI based on hyperoxia. NeuroImage 37, 808–820.

Coghill, R.C., Talbot, J.D., Evans, A.C., Meyer, E., Gjedde, A., Bushnell, M.C., Duncan, G.H., 1994. Distributed processing of pain and vibration by the human brain. J. Neurosci. 14, 4095–4108.

Davis, T.L., Kwong, K.K., Weisskoff, R.M., Rosen, B.R., 1998. Calibrated functional MRI: mapping the dynamics of oxidative metabolism. Proc. Natl. Acad. Sci. U. S. A. 95, 1834–1839.

Evans, K.C., Banzett, R.B., Adams, L., McKay, L., Frackowiak, R.S., Corfield, D.R., 2002. BOLD fMRI identifies limbic, paralimbic, and cerebellar activation during air hunger. J. Neurophysiol. 88, 1500–1511.

Fernandez-Seara, M.A., Edlow, B.L., Hoang, A., Wang, J., Feinberg, D.A., Detre, J.A., 2008. Minimizing acquisition time of arterial spin labeling at 3T. Magn. Reson. Med. 59, 1467–1471.

Fox, P.T., Raichle, M.E., 1984. Stimulus rate dependence of regional cerebral blood flow in human striate cortex, demonstrated by positron emission tomography. J. Neurophysiol. 51, 1109–1120.

Fox, P.T., Raichle, M.E., 1986. Focal physiological uncoupling of cerebral blood flow and oxidative metabolism during somatosensory stimulation in human subjects. Proc. Natl. Acad. Sci. U. S. A. 83, 1140–1144.

Fox, P.T., Raichle, M.E., Mintun, M.A., Dence, C., 1988. Nonoxidative glucose consumption during focal physiologic neural activity. Science 241, 462–464.

Frackowiak, R.S., Lenzi, G.L., Jones, T., Heather, J.D., 1980. Quantitative measurement of regional cerebral blood flow and oxygen metabolism in man using 15O and positron emission tomography: theory, procedure, and normal values. J. Comput. Assist. Tomogr. 4, 727–736.

Gauthier, C., Hoge, R.D., 2011a. A generalized procedure for calibrated MRI incorporating hyperoxia and hypercapnia. Hum. Brain Mapp.

Gauthier, C.J., Hoge, R.D., 2011b. Magnetic resonance imaging of resting OEF and CMRO(2) using a generalized calibration model for hypercapnia and hyperoxia. NeuroImage 54, 1001–1011.

Gauthier, C.J., Madjar, C., Tancredi, F.B., Stefanovic, B., Hoge, R.D., 2011. Elimination of visually evoked BOLD responses during carbogen inhalation: implications for calibrated MRI. NeuroImage 54, 1001–1011.

Glover, G.H., Li, T.Q., Ress, D., 2000. Image-based method for retrospective correction of physiological motion effects in fMRI: RETROICOR. Magn. Reson. Med. 44, 162–167.

Goodwin, J.A., Vidyasagar, R., Balanos, G.M., Bulte, D., Parkes, L.M., 2009. Quantitative fMRI using hyperoxia calibration: reproducibility during a cognitive Stroop task. NeuroImage 47, 573–580.

Griffeth, V.E., Buxton, R.B., 2011. A theoretical framework for estimating cerebral oxygen metabolism changes using the calibrated-BOLD method: modeling the effects of blood volume distribution, hematocrit, oxygen extraction fraction, and tissue signal properties on the BOLD signal. NeuroImage 58, 198–212.

Grubb Jr., R.L., Raichle, M.E., Eichling, J.O., Ter-Pogossian, M.M., 1974. The effects of changes in PaCO2 on cerebral blood volume, blood flow, and vascular mean transit time. Stroke 5, 630–639.

He, X., Yablonskiy, D.A., 2007. Quantitative BOLD: mapping of human cerebral deoxygenated blood volume and oxygen extraction fraction: default state. Magn. Reson. Med. 57, 115–126.

He, X., Zhu, M., Yablonskiy, D.A., 2008. Validation of oxygen extraction fraction measurement by qBOLD technique. Magn. Reson. Med. 60, 882–888.

Hino, J.K., Short, B.L., Rais-Bahrami, K., Seale, W.R., 2000. Cerebral blood flow and metabolism during and after prolonged hypercapnia in newborn lambs. Crit. Care Med. 28, 3505–3510.

Hoge, R.D., Atkinson, J., Gill, B., Crelier, G.R., Marrett, S., Pike, G.B., 1999a. Investigation of BOLD signal dependence on cerebral blood flow and oxygen consumption: the deoxyhemoglobin dilution model. Magn. Reson. Med. 42, 849–863.

Hoge, R.D., Atkinson, J., Gill, B., Crelier, G.R., Marrett, S., Pike, G.B., 1999b. Linear coupling between cerebral blood flow and oxygen consumption in activated human cortex. Proc. Natl. Acad. Sci. U. S. A. 96, 9403–9408.

Horvath, I., Sandor, N.T., Ruttner, Z., McLaughlin, A.C., 1994. Role of nitric oxide in regulating cerebrocortical oxygen consumption and blood flow during hypercapnia. J. Cereb. Blood Flow Metab. 14, 503–509.

Jezzard, P., Heineman, F., Taylor, J., DesPres, D., Wen, H., Balaban, R.S., Turner, R., 1994. Comparison of EPI gradient-echo contrast changes in cat brain caused by respiratory challenges with direct simultaneous evaluation of cerebral oxygenation via a cranial window. NMR Biomed. 7, 35–44.

Jones, M., Berwick, J., Hewson-Stoate, N., Gias, C., Mayhew, J., 2005. The effect of hypercapnia on the neural and hemodynamic responses to somatosensory stimulation. NeuroImage 27, 609–623.

Kida, I., Kennan, R.P., Rothman, D.L., Behar, K.L., Hyder, F., 2000. High-resolution CMR(O2) mapping in rat cortex: a multiparametric approach to calibration of BOLD image contrast at 7 Tesla. J. Cereb. Blood Flow Metab. 20, 847–860.

Kuwabara, H., Ohta, S., Brust, P., Meyer, E., Gjedde, A., 1992. Density of perfused capillaries in living human brain during functional activation. Prog. Brain Res. 91, 209–215.

Leontiev, O., Buxton, R.B., 2007. Reproducibility of BOLD, perfusion, and CMRO2 measurements with calibrated-BOLD fMRI. NeuroImage 35, 175–184.

Leontiev, O., Dubowitz, D.J., Buxton, R.B., 2007. CBF/CMRO2 coupling measured with calibrated BOLD fMRI: sources of bias. NeuroImage 36, 1110–1122.

Lu, H., Golay, X., Pekar, J.J., Van Zijl, P.C., 2003. Functional magnetic resonance imaging based on changes in vascular space occupancy. Magn. Reson. Med. 50, 263–274.

Luh, W.M., Wong, E.C., Bandettini, P.A., Hyde, J.S., 1999. QUIPSS II with thin-slice TI1 periodic saturation: a method for improving accuracy of quantitative perfusion imaging using pulsed arterial spin labeling. Magn. Reson. Med. 41, 1246–1254.

Malonek, D., Dirnagl, U., Lindauer, U., Yamada, K., Kanno, I., Grinvald, A., 1997. Vascular imprints of neuronal activity: relationships between the dynamics of cortical blood flow, oxygenation, and volume changes following sensory stimulation. Proc. Natl. Acad. Sci. U. S. A. 94, 14826–14831.

Mandeville, J.B., Marota, J.J., Ayata, C., Moskowitz, M.A., Weisskoff, R.M., Rosen, B.R., 1999. MRI measurement of the temporal evolution of relative CMRO(2) during rat forepaw stimulation. Magn. Reson. Med. 42, 944–951.

Marrett, S., Gjedde, A., 1997. Changes of blood flow and oxygen consumption in visual cortex of living humans. Adv. Exp. Med. Biol. 413, 205–208.

McPherson, R.W., Derrer, S.A., Traystman, R.J., 1991. Changes in cerebral CO2 responsivity over time during isoflurane anesthesia in the dog. J. Neurosurg. Anesthesiol. 3, 12–19.

Mohtasib, R.S., Lumley, G., Goodwin, J.A., Emsley, H.C., Sluming, V., Parkes, L.M., 2012. Calibrated fMRI during a cognitive Stroop task reveals reduced metabolic response with increasing age. NeuroImage 59, 1143–1151.

Obata, T., Liu, T.T., Miller, K.L., Luh, W.M., Wong, E.C., Frank, L.R., Buxton, R.B., 2004. Discrepancies between BOLD and flow dynamics in primary and supplementary motor areas: application of the balloon model to the interpretation of BOLD transients. NeuroImage 21, 144–153.

Ogawa, S., Lee, T.M., Nayak, A.S., Glynn, P., 1990. Oxygenation-sensitive contrast in magnetic resonance image of rodent brain at high magnetic fields. Magn. Reson. Med. 14, 68–78.

Ogawa, S., Menon, R.S., Tank, D.W., Kim, S.G., Merkle, H., Ellermann, J.M., Ugurbil, K., 1993. Functional brain mapping by blood oxygenation level-dependent contrast magnetic resonance imaging. A comparison of signal characteristics with a biophysical model. Biophys. J. 64, 803–812.

Ohta, S., Meyer, E., Thompson, C.J., Gjedde, A., 1992. Oxygen consumption of the living human brain measured after a single inhalation of positron emitting oxygen. J. Cereb. Blood Flow Metab. 12, 179–192.

Perthen, J.E., Lansing, A.E., Liau, J., Liu, T.T., Buxton, R.B., 2008. Caffeine-induced uncoupling of cerebral blood flow and oxygen metabolism: a calibrated BOLD fMRI study. NeuroImage 40, 237–247.

Raichle, M.E., Grubb Jr., R.L., Gado, M.H., Eichling, J.O., Ter-Pogossian, M.M., 1976. Correlation between regional cerebral blood flow and oxidative metabolism. In vivo studies in man. Arch. Neurol. 33, 523–526.

Redies, C., Hoffer, L.J., Beil, C., Marliss, E.B., Evans, A.C., Lariviere, F., Marrett, S., Meyer, E., Diksic, M., Gjedde, A., et al., 1989. Generalized decrease in brain glucose metabolism during fasting in humans studied by PET. Am. J. Physiol. 256, E805–E810.

Restom, K., Perthen, J.E., Liu, T.T., 2008. Calibrated fMRI in the medial temporal lobe during a memory-encoding task. NeuroImage 40, 1495–1502.

Tancredi FB, G.C., Madjar C, Bolard DS, Fisher J, Wang DJ, Hoge RD, In Press. Comparison of pulsed and pseudo-continuous arterial spin-labeling for measuring CO2-induced cerebrovascular reactivity. JMRI.

Vafaee, M.S., Meyer, E., Marrett, S., Paus, T., Evans, A.C., Gjedde, A., 1999. Frequency-dependent changes in cerebral metabolic rate of oxygen during activation of human visual cortex. J. Cereb. Blood Flow Metab. 19, 272–277.

Weisskoff, R.M., Zuo, C.S., Boxerman, J.L., Rosen, B.R., 1994. Microscopic susceptibility variation and transverse relaxation: theory and experiment. Magn. Reson. Med. 31, 601–610.

Wong, E.C., Buxton, R.B., Frank, L.R., 1997. Implementation of quantitative perfusion imaging techniques for functional brain mapping using pulsed arterial spin labeling. NMR Biomed. 10, 237–249.

Wong, E.C., Buxton, R.B., Frank, L.R., 1998. A theoretical and experimental comparison of continuous and pulsed arterial spin labeling techniques for quantitative perfusion imaging. Magn. Reson. Med. 40, 348–355.

Wu, W.C., Fernandez-Seara, M., Detre, J.A., Wehrli, F.W., Wang, J., 2007. A theoretical and experimental investigation of the tagging efficiency of pseudocontinuous arterial spin labeling. Magn. Reson. Med. 58, 1020–1027.

Wu, W.C., Edlow, B.L., Elliot, M.A., Wang, J., Detre, J.A., 2009. Physiological modulations in arterial spin labeling perfusion magnetic resonance imaging. IEEE Trans. Med. Imaging 28, 703–709.

Xu, F., Uh, J., Brier, M.R., Hart Jr., J., Yezhuvath, U.S., Gu, H., Yang, Y., Lu, H., 2011. The influence of carbon dioxide on brain activity and metabolism in conscious humans. J. Cereb. Blood Flow Metab. 31, 58–67.

Yablonskiy, D.A., Haacke, E.M., 1994. Theory of NMR signal behavior in magnetically inhomogeneous tissues: the static dephasing regime. Magn. Reson. Med. 32, 749–763.

Yasaka, M., Read, S.J., O'Keefe, G.J., Egan, G.F., Pointon, O., McKay, W.J., Donnan, G.A., 1998. Positron emission tomography in ischaemic stroke: cerebral perfusion and metabolism after stroke onset. J. Clin. Neurosci. 5, 413–416.

Zappe, A.C., Uludag, K., Oeltermann, A., Ugurbil, K., Logothetis, N.K., 2008. The influence of moderate hypercapnia on neural activity in the anesthetized nonhuman primate. Cereb. Cortex 18, 2666–2673.

Zatorre, R.J., Evans, A.C., Meyer, E., Gjedde, A., 1992. Lateralization of phonetic and pitch discrimination in speech processing. Science 256, 846–849.